J Neurophysiol 94: 1554–1564, 2005.
First published April 13, 2005; doi:10.1152/jn.00299.2005.

Monoaminergic Establishment of Rostrocaudal Gradients of Rhythmicity in the Neonatal Mouse Spinal Cord

Kimberly J. Christie[1,2] and Patrick J. Whelan[1,2,3]

[1]*Hotchkiss Brain Institute,* [2]*Department of Physiology and Biophysics, and* [3]*Department of Clinical Neurosciences, University of Calgary, Calgary, Alberta, Canada*

Submitted 21 March 2005; accepted in final form 11 April 2005

Christie, Kimberly J. and Patrick J. Whelan. Monoaminergic establishment of rostrocaudal gradients of rhythmicity in the neonatal mouse spinal cord. *J Neurophysiol* 94: 1554–1564, 2005. First published April 13, 2005; doi:10.1152/jn.00299.2005. Bath application of monoamines is a potent method for evoking locomotor activity in neonatal rats and mice. Monoamines also promote functional recovery in adult animals with spinal cord injuries by activating spinal cord networks. However, the mechanisms of their actions on spinal networks are largely unknown. In this study, we tested the hypothesis that monoamines establish rostrocaudal gradients of rhythmicity in the thoracolumbar spinal cord. Isolated neonatal mouse spinal cord preparations (P0–P2) were used. To assay excitability of networks by monoamines, we evoked a disinhibited rhythm by bath application of picrotoxin and strychnine and recorded neurograms from several thoracolumbar ventral roots. We first established that rostral and caudal segments of the thoracolumbar spinal cord had equal excitability by completely transecting preparations at the L_3 segmental level and recording the frequency of the disinhibited rhythm from both segments. Next we established that a majority of ventral interneurons retrogradely labeled by calcium green dextran were active during network activity. We then bath applied combinations of monoaminergic agonists [5-HT and dopamine (DA)] known to elicit locomotor activity. Our results show that monoamines establish rostrocaudal gradients of rhythmicity in the thoracolumbar spinal cord. This may be one mechanism by which combinations of monoaminergic compounds normally stably activate locomotor networks.

INTRODUCTION

Several laboratories using the neonatal mouse or rat preparation have shown that combinations of monoamines with *N*-methyl-D(L)-aspartic acid [NMA/*N*-methyl-D-aspartate (NMDA)] are effective in evoking sustained bouts of network activity (Barriere et al. 2004; Jiang et al. 1999a,b; Madriaga et al. 2004; Nishimaru et al. 2000; Schmidt and Jordan 2000; Smith et al. 1988; Sqalli-Houssaini and Cazalets 2000; Sqalli-Houssaini et al. 1993; Whelan et al. 2000). It is a matter of debate why certain monoamine combinations are so effective in promoting activation of developing locomotor networks. In all likelihood, a combination of receptor distribution, intrinsic cellular properties, and network properties all contribute to the rhythmogenic potential of monoamines such as 5-HT and dopamine (DA). One possibility is that the distribution of 5-HT and DA receptors in the rostrocaudal axis may be conducive to the formation of functional gradients of neuronal excitability. Gradients of excitability are known to be important for network function (Iizuka 2004; Kiemel et al. 2003; Matsushima and Grillner 1992). Gradients contribute to the temporal sequencing of segmental activity, thus affecting the behavior of the animal. In the case of the lamprey, dogfish, and xenopus (Cohen 1987; Hagevik and McClellan 1999; Matsushima and Grillner 1990; Roberts and Tunstall 1994; Tunstall and Roberts 1994), rostrocaudal gradients also contribute to the generation of an intersegmental phase lag, and in lamprey, is considered crucial for generation of an S-shaped swim pattern (Grillner 2003). In mammals, gradients of excitability could affect activity-dependent development of spinal circuits and may impose a rudimentary organization over the sequencing of rhythmic movements.

Several lines of evidence suggest that mammalian locomotor networks have a rostrocaudal gradient of activity (Bertrand and Cazalets 2002; Bonnot et al. 2002b; Cowley and Schmidt 1997; Kiehn and Kjaerulff 1998). Paradoxically, one of the complexities in establishing whether monoamines set up rostrocaudal gradients of neuronal excitability is that they effectively activate locomotor networks. Evidence from the neonatal mouse suggests that rostrocaudal gradients of activity may partly be an emergent property of locomotor networks (Bonnot et al. 2002b). One possible method to examine whether monoamines set up excitability gradients would be to manipulate a spinal central pattern generator (CPG) that does not exhibit a rostrocaudal gradient of excitability.

In this paper, we take advantage of a rhythm evoked by blocking inhibitory drive (Bracci et al. 1996a,b, 1997; Cowley and Schmidt 1995; Jiang et al. 1999b) that does not normally show a rostrocaudal gradient of excitability. There are several additional advantages afforded when using a purely excitatory network to examine rostrocaudal gradients. First, it constrains the mechanisms of action of monoamines. Second, evidence from neonatal rat preparations suggests that purely excitatory spinal networks share circuitry used in the generation of locomotor-like rhythms (Beato and Nistri 1999; Bracci et al. 1996a).

In this paper, we test the hypothesis that combinations of monoamines that effectively elicit bouts of locomotor activity promote rostrocaudal gradients of excitability. A portion of these results have been published in abstract form (Christie and Whelan 2004).

METHODS

Experiments were performed on Swiss Webster mice (Charles River Laboratories), 0–2 days old (P0–P2; $n = 58$). All procedures

Address for reprint requests and other correspondence: P. J. Whelan, HSC 2119, Dept. of Physiology and Biophysics, Univ. of Calgary, Calgary, AB T2N 4N1, Canada (E-mail: whelan@ucalgary.ca).

The costs of publication of this article were defrayed in part by the payment of page charges. The article must therefore be hereby marked "*advertisement*" in accordance with 18 U.S.C. Section 1734 solely to indicate this fact.

were approved by the University of Calgary Animal Care Committee. The animals were anesthetized by hypothermia, decapitated, and eviscerated. The tissue was pinned in a sylgard-lined dissection chamber filled with oxygenated (95% O_2-5% CO_2) artificial cerebrospinal fluid (ACSF; concentrations in mM: 128 NaCl, 4 KCl, 1.5 $CaCl_2$, 1 $MgSO_4$, 0.5 Na_2HPO_4, 21 $NaHCO_3$, and 30 D-glucose). A ventral laminectomy exposed the spinal cord, and the ventral and dorsal roots were cut. The spinal cord was transected at thoracic segment 5 (T_5) to the cauda equina and gently removed from the vertebral column. After 30 min, the spinal cord was transferred to the recording chamber and superfused with oxygenated ACSF. The bath solution was heated gradually from room temperature (~20–22°C) to 27°C. The preparation was allowed to equilibrate for another hour in the recording chamber.

Neurograms were recorded using suction electrodes into which segmental ventral roots T_{12}, T_{13}, Lumbar 2 (L_2), L_4 from the left side and both L_5s were drawn. Strychnine hydrochloride (10 μM; Sigma-Aldrich) and picrotoxin (50 μM; Sigma-Aldrich) were added to the bath, which resulted in synchronous bursting throughout all ventral roots. The rhythm was allowed to stabilize for 30 min after which the cycle period, calculated as the time between successive bursts, was averaged over a 10-min interval. After this period of time, monoaminergic agonists were added. In certain experiments, the spinal cord was completely transected at L_3, and the rostral and caudal cycle periods were compared.

Electrophysiological recordings

Neurogram recordings were amplified (100–20,000 times), bandpass filtered (100 Hz to 1 kHz or DC to 1 kHz; these settings allowed slow potentials and propagated spike activity to be resolved), and digitized at 2 kHz (Axon Digidata 1320) for future analyses. All off-line analyses were performed using custom-designed MatLab programs that directly imported the digitized Axon files.

The data were low-pass filtered using a Gaussian filter at 10 Hz and decimated by a reduction factor of 50. The first derivative of the filtered and decimated data were calculated to determine burst initiation points. Bursts were easily detected using this algorithm since sharp increases in slope occurred during burst onset (Fig. 1*B*). We arbitrarily set the burst initiation point as one-sixth of the maximum amplitude of the differentiated trace. This initiation point was chosen as the one that produced the most reliable detection of burst events. The cycle period was determined by subtracting the times between successive burst initiation points. The phase lag between bursts in T_{13} and L_5 was calculated by averaging bursts detected using the above algorithm from a 5-min stretch of data with ~8–10 bursts. Phase lags between adjacent roots were calculated by first taking the averaged bursts from T_{13} and L_5 and aligning each to zero to remove offsets and normalizing the amplitudes. A cross-correlogram between the two averaged bursts was calculated, the number of lags from zero to the maximum correlation coefficient was measured, and the resultant phase lag was expressed in milliseconds. The phase lag was divided by the average cycle period for that 5-min stretch of data to give a normalized phase lag. Statistical comparisons between experimental conditions were made using one-way ANOVAs if the data were normally distributed and had equal variance. Otherwise, the data were compared with a Kruskal-Wallis rank sum test.

Imaging experiments

DYE LOADING. In three experiments, ventral interneurons in the L_{1-2} segments were retrogradely loaded with calcium green dextran dye (10,000 MW; Molecular Probes, Eugene, OR) using established techniques (Bonnot et al. 2002a,b; O'Donovan et al. 1993). A suction electrode (PE 90) was positioned ventromedially, and a small section of white matter was drawn up into the electrode. The electrode was filled with dye (10 mM) dissolved in 0.2% Triton X-100 (6 μl). The cord was left for 12–14 h in ice-cold ACSF that was allowed to warm up to room temperature to allow retrograde loading of cell bodies.

OPTICAL IMAGING. The cord was transversely sectioned, and the rostral or caudal sections were pinned upright onto a sylgard wedge

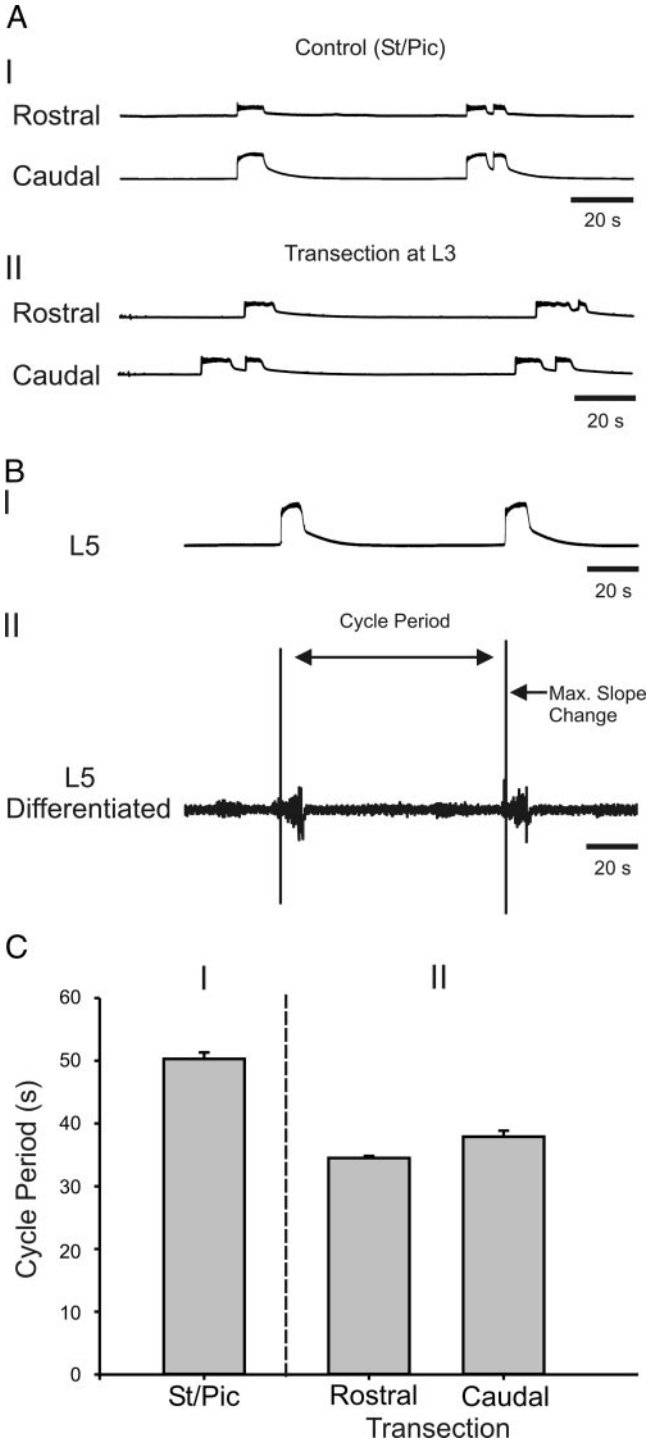

FIG. 1. Rhythm evoked with strychnine and picrotoxin. *AI*: neurogram showing synchronous bursting with 10 μM strychnine and 50 μM picrotoxin from T_{12} ventral root (*top*) and L_5 ventral root (*bottom*). *AII*: after a transection at L_3. *BI*: neurogram from L_5 ventral root with strychnine and picrotoxin. *BII*: differential of data from *BI* shows how cycle period was calculated. *CI*: average cycle period for strychnine and picrotoxin rhythm ($n = 58$). *CII*: average cycle periods from a rostral ventral root compared with a caudal root after a transection at L_3 ($n = 11$).

anchored to a coverslip by petroleum jelly (Fig. 2). The petroleum jelly allowed the wedge to be easily maneuvered into position. The cord was placed in a chamber on an inverted epifluorescence microscope (Zeiss Axiovert) and continuously perfused with ACSF. The tissue was illuminated by a 75-W mercury light source (excitation filter, 470–490 nm; emission filter, 520–560 nm), and labeled interneurons were visualized. Activity-dependent changes in fluorescence were detected using an intensified CCD camera (Stanford Photonics, Salt Lake City, UT), digitized on a Dazzle (A/D converter), and stored on the hard drive using Adobe Premiere. Changes in fluorescence were monitored on-line using an imaging processing unit (Hamamatsu Photonics, Hamamatsu City, Japan). Image-processing software was used to analyze the data (Metamorph, Universal Imaging, West Chester, PA). In brief, regions of interest (ROIs) were placed around ventrally labeled interneurons, and changes in average pixel intensity were quantified before and during an episode of activity by dividing the change in fluorescence by the background ($\%\Delta F/F$). The optical and electrophysiological data were synchronized using two pulses separated by ~6–8 s. These pulses were recorded onto a digitizer channel and through an audio track of the Dazzle A/D converter. As a result, optical and electrophysiological traces were synchronized off-line.

Pharmacology

Pharmacological reagents used in this study included strychnine hydrochloride (glycine receptor antagonist, 10 μM, Sigma-Aldrich), picrotoxin ($GABA_A$ receptor antagonist, 50 μM, Sigma-Aldrich), dopamine hydrochloride (DA, 50, 75, and 100 μM, Sigma-Aldrich), SKF 81297 hydrobromide (D_1 receptor agonist, 20 μM, Sigma-Aldrich), quinpirole hydrochloride (D_2 receptor agonist, 40 μM, Sigma-Aldrich), serotonin hydrochloride (5-HT, 10, 15, and 30 μM, Sigma-Aldrich), α-methyl-5-hydroxytryptamine ($5\text{-}HT_2$ receptor agonist, 4 μM, Sigma-Aldrich), and *N*-methyl-DL-aspartic acid (NMA, 5 μM, Sigma-Aldrich).

RESULTS

Our main goal was to establish whether monoamines that commonly elicit locomotor activity contribute to the establishment of gradients of excitability within the thoracolumbar spinal cord. We made use of a disinhibited rhythm that is evoked after administration of $GABA_A$ (picrotoxin) and glycinergic (strychnine) antagonists. We first established that without monoamines in the bath, this rhythm does not have a rostrocaudal gradient of excitability and that a majority of retrogradely labeled ventral interneurons were activated during an episode. Next we established whether monoaminergic agonists commonly used to elicit locomotor activity produced rostrocaudal gradients.

Evoked rhythm

Figure 1*A* shows the bursting pattern from T_{12} and L_5 ventral root neurograms after bath application of 10 μM strychnine and 50 μM picrotoxin. A stable rhythm was generally established after 15–30 min of drug application, which was synchronous across all neurograms. On average, the cycle period was 50 ± 7.78 (SD) s (range, 30–60 s; $n = 58$), and an average burst was 4–6 s in length. On occasion, several multi-cycle slow bursts would appear (Fig. 1*A*). We did not generally observe multi-cycle fast oscillations superimposed on each episode as reported for the isolated rat spinal cord preparation (Bracci et al. 1996a).

In a separate set of experiments, we tested whether a rostrocaudal gradient of excitability exists between rostral thoracolumbar and caudal lumbosacral segments. A synchronous rhythm was evoked, and after 10 min of recording control activity, the spinal cord preparations were completely transected at the L_3 segmental level (Fig. 1). Before the transection, the average cycle period was 40 s. After the transection, the rhythm continued after a short break of 1–2 min without a significant difference between the rostral (35 s) and caudal (38 s) segments ($n = 11$). The burst duration decreased by 1–2 s in the rostral and caudal segments after the transection.

Although it is assumed that ventral interneurons in lamina VII and VIII are activated during disinhibited network activity, this has not been tested directly. We tested this by retrogradely labeling populations of ventral commissural and ipsilateral projecting interneurons with calcium green dextran dye in three spinal cord preparations. As indicated by Fig. 2, cells labeled by this technique were generally found in lamina VII and VIII. Neurogram recordings were also made to complement the optical recordings. Recordings were made from a total of 15 loaded cells visible at the transverse surface. Eleven of 15 of these cells were activated during an electrically recorded episode (see Fig. 2). Retrogradely labeled interneurons (Fig. 2*C*) showed an increase in calcium transients in phase with neurogram ventral root bursts. Previous work has established that these types of calcium transients are a reflection of spike activity within motoneurons (Bonnot et al. 2005; O'Donovan et al. 1993).

Effects of DA and 5-HT on the disinhibited rhythm

DOPAMINE. Bath application of DA (50 and 100 μM) to a disinhibited rhythm evoked with strychnine and picrotoxin caused an increase in the population motoneuronal potential, which often led to an increase in overall tonic bursting that reached a plateau ~5–10 min later (Fig. 3). This increase in DC potential was accompanied by a significant decrease of 30 and 47%, respectively, in the cycle period ($P < 0.05$; $n = 10$, $n = 6$; Fig. 3). While synchronous rhythmic activity was usually observed, mini-bursts were found in 3/10 of the cords treated with 100 μM DA (Fig. 3*AIII*). These mini-bursts were found in T_{12}, T_{13}, and L_2 ventral roots, but not in caudal lumbar segments, and were uncoupled from the large bursts. These bursts were never observed during the administration of low concentrations of dopamine (50 μM) in the presence of strychnine and picrotoxin. Bath application of specific D_1 (SKF 81297) and D_2 (quinpirole) receptor agonists also significantly decreased the cycle period (60% reduction; $P < 0.05$; $n = 7$; Fig. 3). In separate experiments, bath application of SKF 81297 alone resulted in a decrease in the cycle period (40% reduction; $P < 0.05$, $n = 6$; data not shown).

After a complete transection at the L_3 segment, the bursting from rostral segments was more frequent than that in caudal segments (50 and 100 μM DA; $P < 0.05$; $n = 6$; $n = 10$; Fig. 4). It is conceivable that increased activity of neurons after bath application of DA may have boosted injury potentials after a transection of the spinal cord. To control for this possibility, in a separate set of experiments, we first transected the spinal cords and then added DA. Bath application of DA (100 μM) after the transection at L_3 also resulted in bursts occurring more

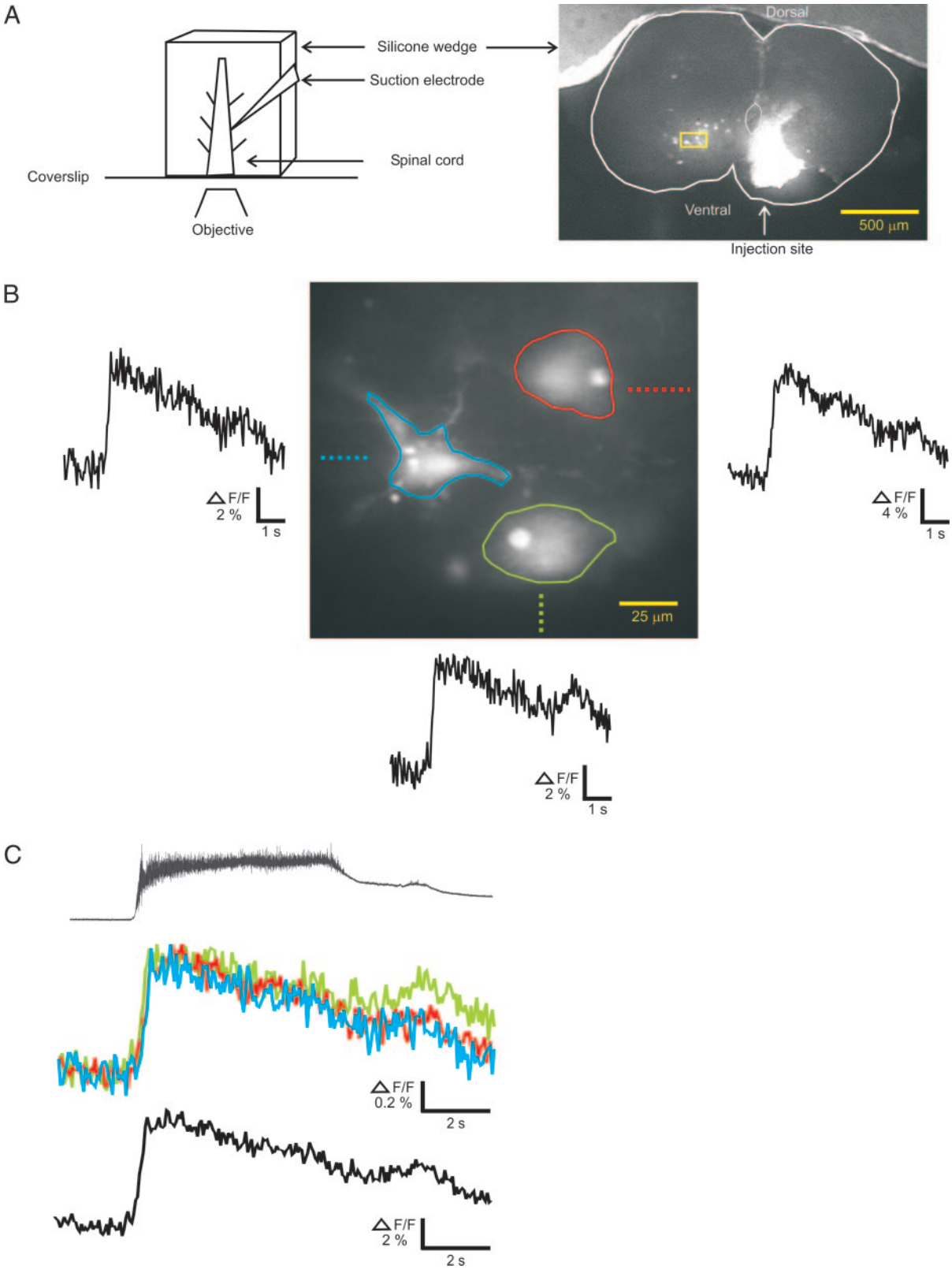

FIG. 2. Calcium transients recorded from ventral interneurons. *A*: *left*: schematic of experimental setup. Cord is pinned to a sylgard wedge positioned over the coverslip. *Right*: raw fluorescence image of transverse surface of neonatal mouse spinal cord (×5). Box indicates position of contralateral cells shown in *B*. Injection site of dye is indicated by arrow. Central canal is also outlined. *B*: fluorescence image with 3 selected regions surrounding the 3 cells where calcium transients were monitored (×40). *C*: *top*: neurogram recorded from a ventral root of the burst. *Middle*: calcium transients from selected regions (color matched to *B*). *Bottom*: average trace obtained from all 3 regions of interest.

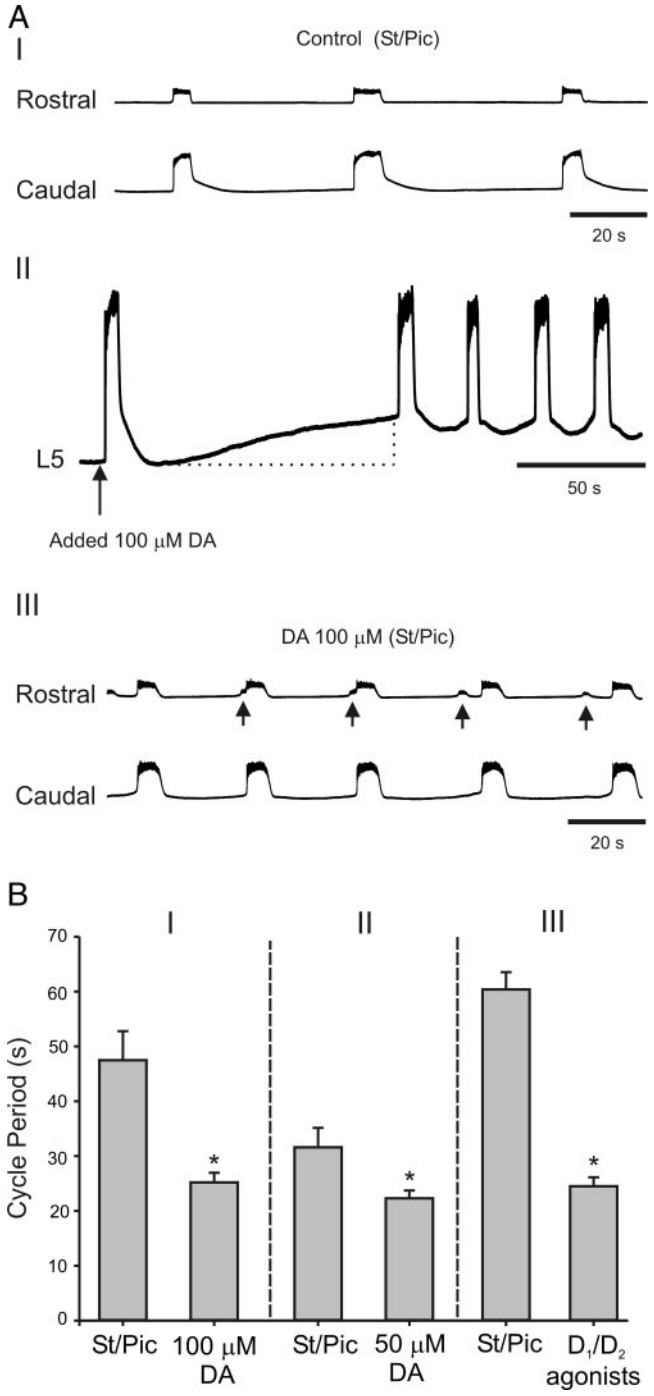

FIG. 3. Dopamine (DA) decreases cycle period of a strychnine- and picrotoxin-evoked rhythm. *AI*: rhythm evoked with strychnine (10 μM) and picrotoxin (50 μM), recordings from T_{12} (*top*) and L_5 (*bottom*) ventral roots. *AII*: increase in DC potential after addition of 100 μM DA, shown in L_5 ventral root. *AIII*: bath application of 100 μM DA, arrows indicate mini-bursts. *BI*: summary plot of cycle period decrease with 100 μM DA ($P < 0.05$, $n = 10$). *BII*: summary plot of cycle period decrease with 50 μM DA ($P < 0.05$, $n = 6$). *BIII*: summary plot of cycle period decrease with D_1 and D_2 receptors agonists (20 and 40 μM, respectively; $P < 0.05$, $n = 7$).

frequently in the rostral compared with caudal segments ($P < 0.05$; $n = 5$; data not shown).

Although the addition of D_1 and D_2 receptor agonists decreased the cycle period of the strychnine/picrotoxin rhythm, after transection of the cord, the cycle periods of the rostral and caudal segments were the same ($P = 0.076$; $n = 7$; Fig. 4), suggesting that DA may have been activating a different subset of receptors. Similar results were observed following application of the D_1 receptor agonist alone ($P = 0.884$; $n = 6$; data not shown).

5-HT. Bath application of 10 or 30 μM 5-HT to the strychnine/picrotoxin rhythm increased the underlying DC potential and increased the speed and stability of the rhythm [cycle period decreased by 52 (10 μM 5-HT; $P < 0.05$; $n = 6$) and 63% (30 μM 5-HT; $P < 0.05$; $n = 6$)]. Similar to DA, the burst duration decreased by 2–3 s after bath application of 5-HT. After the transection at L_3, the cycle periods of the rostral and caudal segments remained the same in the presence of 10 μM 5-HT ($P = 1.0$; $n = 6$; Fig. 5, *A* and *B*). However, when we increased the concentration of 5-HT (from 10 to 30 μM 5-HT), the

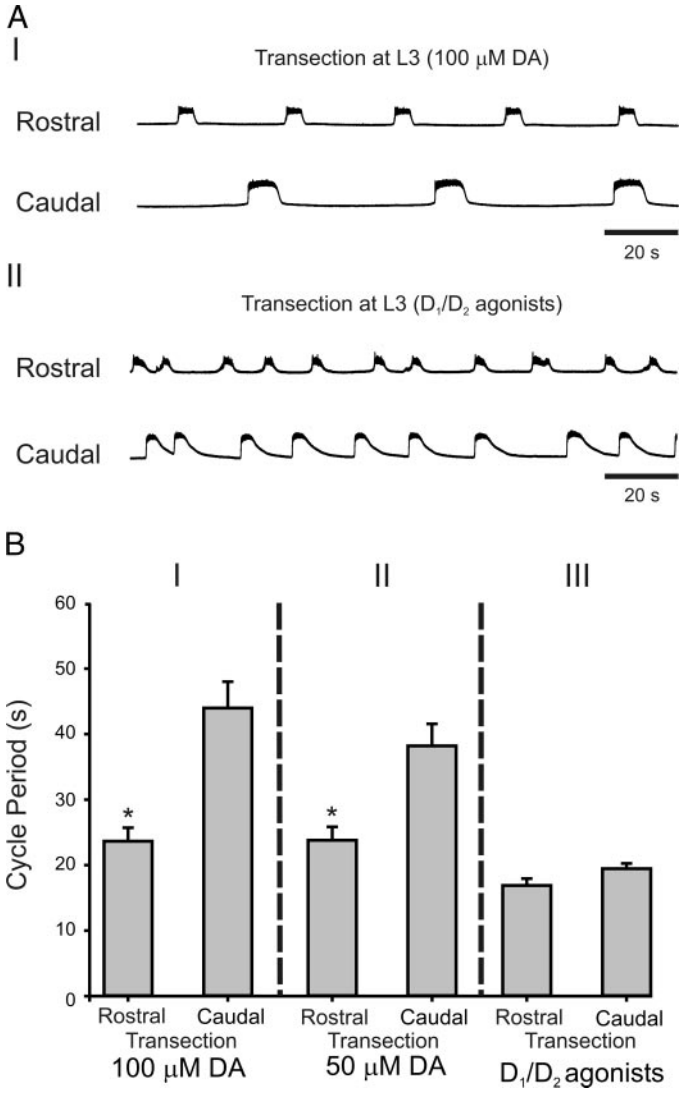

FIG. 4. Effect of DA on cycle periods after a transection. *AI*: neurograms from T_{12} (*top*) and L_5 (*bottom*) ventral roots with 100 μM DA and a complete transection at L_3. *AII*: neurograms from T_{12} (*top*) and L_5 (*bottom*) ventral roots with D_1 (20 μM) and D_2 (40 μM) receptor agonists after a transection at L_3. *BI*: summary plot of cycle periods from rostral and caudal segments with 100 μM DA ($P < 0.05$, $n = 10$). *BII*: summary plot of cycle periods from rostral and caudal segments with 50 μM DA ($P < 0.05$, $n = 6$). *BIII*: summary plot of cycle periods from rostral and caudal segments with D_1 and D_2 receptors agonists (20 and 40 μM, respectively; $P = 0.076$; $n = 7$).

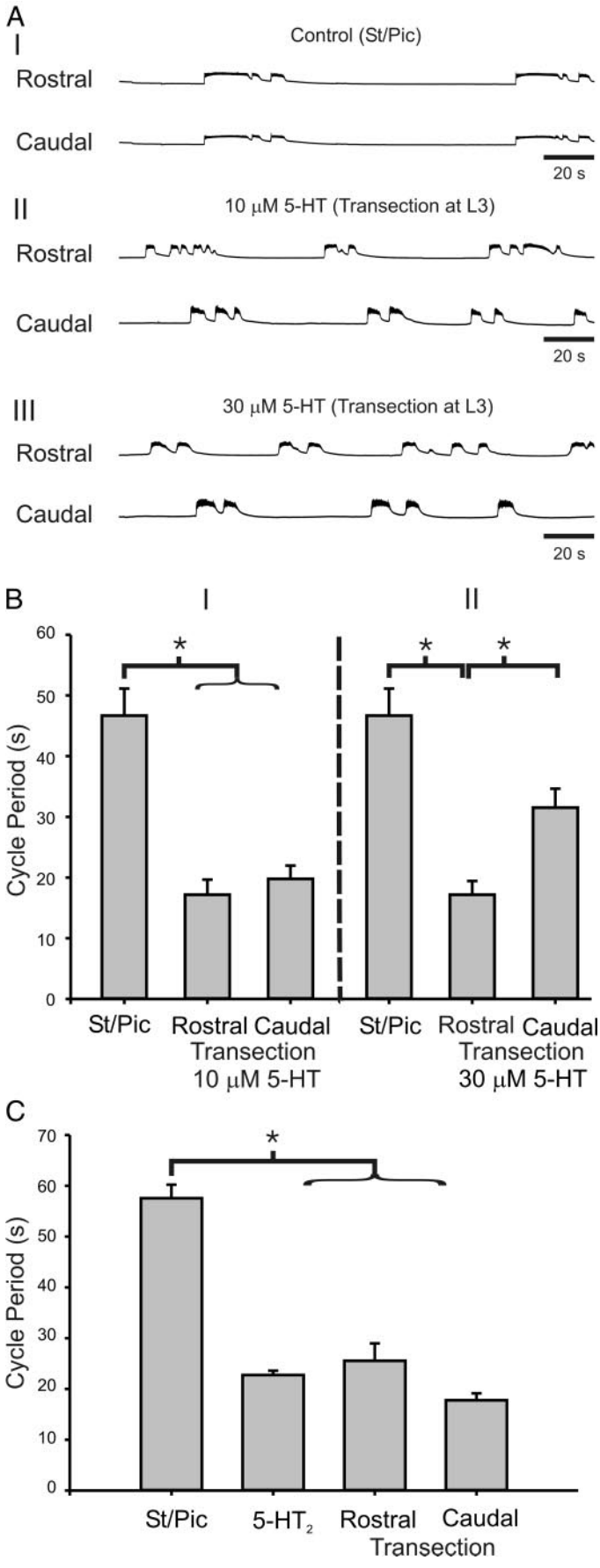

rostral segments started to burst at a faster rate compared with the caudal segments ($P < 0.05$; $n = 6$; Fig. 5, *A* and *B*). In separate experiments, bath application of 4 μM of a 5-HT_2 receptor agonist (α -methyl-5-hydroxytryptamine) increased the rate of bursting (61% reduction in cycle period; $P < 0.05$; $n = 6$). However, no gradient in rostrocaudal excitability was observed after transection of the cord at L_3 ($P = 0.117$; $n = 6$; Fig. 5*C*). Similar to the results for DA, this suggests that 5-HT evokes rostrocaudal gradients of excitability by activation of multiple receptor subtypes.

Combinations that produce locomotion

Normally, combinations of 5-HT, DA, and NMA are extremely effective in eliciting locomotor-like activity in the neonatal mouse preparation. Bath application of NMA, 5-HT, and DA significantly decreased the cycle period by 57% ($P < 0.05$, $n = 5$), and after a transection of the spinal cord, a rostrocaudal gradient in bursting frequency was observed ($P < 0.05$, $n = 5$; Fig. 6, *A* and *D*). Similarly, the combination of 5-HT and DA, which produces a stable locomotor rhythm, decreased the cycle period by 69% ($P < 0.05$, $n = 5$), and after a transection at L_3, the rostral rhythm occurred at a faster rate compared with the caudal segments ($P < 0.05$, $n = 5$; Fig. 6, *B* and *D*). Finally, bath application of D_1, D_2, and 5-HT_2 receptor agonists, which are effective in evoking a locomotor rhythm, resulted in a significant decrease in cycle period of 75% ($P < 0.05$; $n = 8$), and after the transection at L_3, a rostrocaudal gradient of excitability was observed ($P < 0.05$; $n = 8$; Fig. 6, *C* and *D*). All combinations tended to depolarize the population of motoneurons as reflected by the DC potential.

Phase lag

As a result of the significant differences in bursting after a transection, we decided to examine the phase timing of the segments of the intact cord in the presence of combinations of monoamines. Only two of the five combinations showed a small phase lag between T_{13} and L_5 in the intact cord after bath application of monoamines. The evoked rhythm with strychnine and picrotoxin produced a phase of 0.0002, which was significantly smaller than the 0.0007 phase produced with DA/5-HT (75 μM/50 μM; $P < 0.05$, $n = 5$). Similarly, the phase lag produced after application of 5-HT_2/D_1/D_2 (4 μM/20 μM/40 μM; 0.0017) was significantly larger than the control phase lag (0.0003; $P < 0.05$, $n = 8$). All other combinations did not produce a significant phase lag between T_{13} and L_5 [DA (100 μM): $P = 0.074$, $n = 10$; (50 μM): $P = 0.527$, $n =$

FIG. 5. Effects of 5-HT on the cycle period of a strychnine- and picrotoxin-induced rhythm. *AI*: neurograms from T_{12} (*top*) and L_5 (*bottom*) ventral roots with strychnine (10 μM) and picrotoxin (50 μM). *AII*: recordings from T_{12} (*top*) and L_5 (*bottom*) ventral roots with 5-HT (10 μM) receptor agonists after a transection at L_3. *AIII*: recordings from T_{12} (*top*) and L_5 (*bottom*) ventral roots with 5-HT (30 μM) receptor agonists after a transection at L_3. *BI*: summary plot of cycle periods with strychnine and picrotoxin ($P < 0.05$, $n = 6$) and comparing cycle periods from rostral and caudal segments with 10 μM 5-HT ($P = 1.0$, $n = 6$). *BII*: summary plot of cycle periods with strychnine and picrotoxin ($P < 0.05$, $n = 6$) and comparing cycle periods from rostral and caudal segments with 30 μM 5-HT ($P < 0.05$, $n = 6$). *C*: summary plot of cycle periods with strychnine and picrotoxin and 4 μM 5-HT_2 receptor agonist ($P < 0.05$, $n = 6$) and comparing cycle periods from rostral and caudal segments with 4 μM 5-HT_2 receptor agonist ($P = 0.117$, $n = 6$).

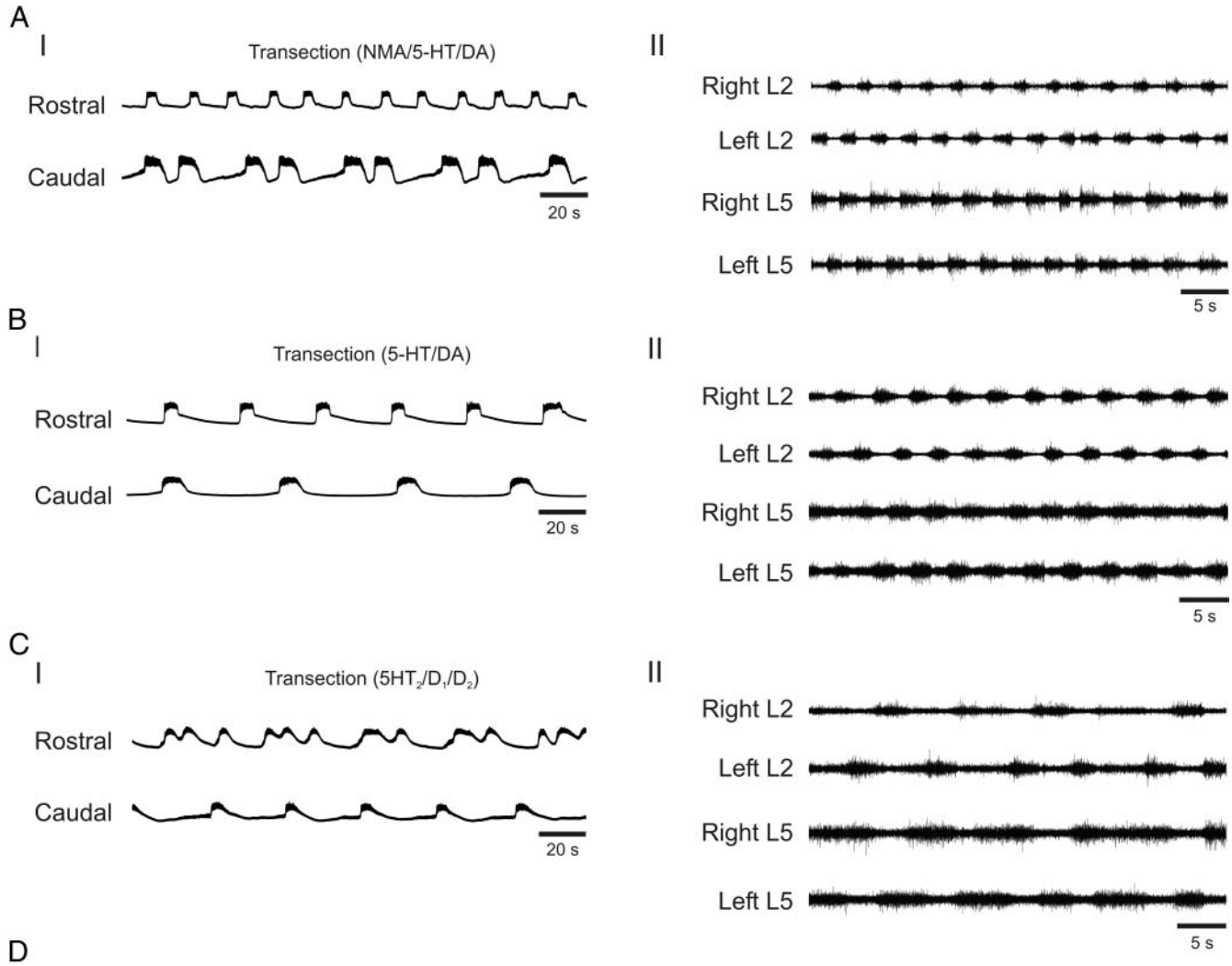

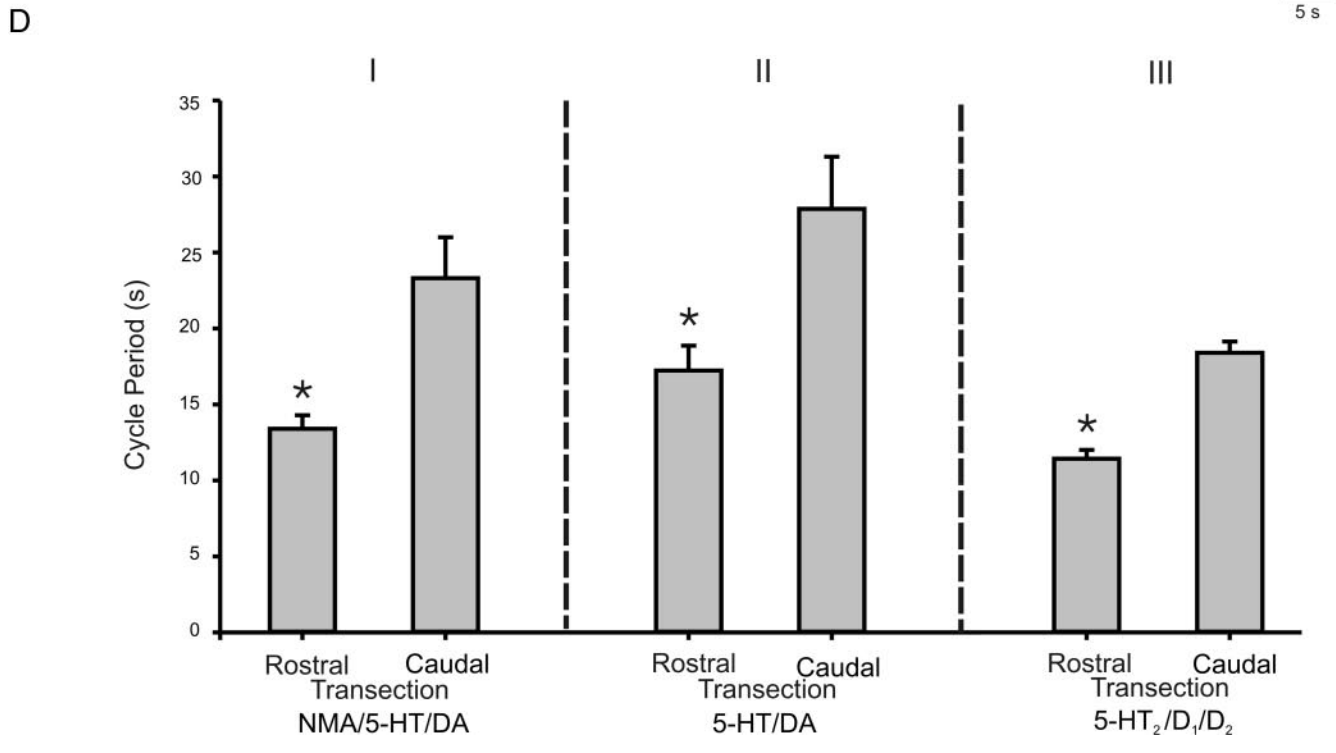

6; NMA/DA/5-HT: $P = 0.365$, $n = 5$; D_1/D_2: $P = 0.07$, $n = 6$; 5-HT_2: $P = 0.137$, $n = 6$].

DISCUSSION

The main result of this paper is that monoamines that generate locomotor activity generate rostrocaudal gradients of excitability in thoracolumbar spinal cord preparations. To assess changes in segmental excitability, we used a disinhibited rhythm evoked by blocking inhibitory conductances. In the mouse, the properties of the bursting dynamics of disinhibited rhythms seem to be essentially the same as reported for the rat (Bracci et al. 1996a,b; Cowley and Schmidt 1995; Kremer and Lev-Tov 1997). We found that the rhythm was coupled with no appreciable phase lag between ipsilateral and segmental roots, as expected for a purely excitatory network with transverse and ipsilateral connectivity. These results are qualitatively similar to those observed using either bicuculline or strychnine in the mouse (Bonnot and Morin 1998). As in the rat, transecting the spinal cord revealed no differences between rostral and caudal rhythm frequency, indicating that the capacity for episodic bursting was distributed in the thoracosacral spinal cord (Bracci et al. 1996a). The rhythm speeds up in a dose-dependent fashion after bath application of NMA, 5-HT, DA, or specific monoaminergic receptor agonists, likely due to depolarization of recurrently connected ventral interneurons (Bracci et al. 1996a). Interestingly, in a minority of preparations, bath application of DA in the presence of strychnine and picrotoxin, evoked two uncoupled rhythms (Fig. 3). A dominant rhythm was evoked across all segments, whereas small mini-bursts could be observed in rostral segments. These mini-bursts were not coupled to the dominant rhythm. One possibility is that these mini-bursts represent activation of a separate network in rostral segments. However, lesion data strongly support the concept of a widely distributed network across thoracolumbar segments (Bonnot and Morin 1998; Bracci et al. 1996a; Kremer and Lev-Tov 1997). Another possibility is that these mini-bursts represent premature activation of rostral segmental networks due to their enhanced excitability. Disinhibited and spontaneously active networks exhibit periods of time after a burst when the network is refractory to bursting (Bracci et al. 1997; O'Donovan 1999). Increased excitation has been shown to reduce this refractory period. Rostral segments, which presumably are more excitable after monoamine application, could activate a portion of the distributed network, resulting in a small burst being evoked. However, because caudal sections are in a refractory state, the burst fails to recruit sufficient recurrently connected neurons in the thoracolumbar network to initiate a full-blown episode. One hypothesis arising from this assumption would be that increased rostral excitability shifts the ignition point of network activity from a presumably stochastic initiation pattern to a pattern of initial activation more localized to T_{11-13} segments. If this hypothesis were supported, these putative shifts in the locus of rostrocaudal network activation would be conceptually similar to findings in the embryonic chick where the locus of spontaneous episode generation in the transverse face shifts to a stochastic pattern when certain interneuronal populations are pharmacologically removed from the network (Wenner and O'Donovan 2001).

Our results indicate that combinations of monoamines that stably activate locomotor networks reliably promote the establishment of a rostrocaudal gradient of excitability in disinhibited networks (Fig. 7). Those monoaminergic receptor agonists, which in our hands, are less effective (D_1/D_2 or 5-HT; <20 μM) in evoking locomotor activity (Madriaga et al. 2004), tend to uniformly increase the excitability of disinhibited thoracolumbar networks. We are interpreting this to indicate that a greater population of interneurons in rostral thoracolumbar compared with caudal lumbosacral segments are recruited by rhythmogenic combinations of monoamines. Rhythms reliant on excitatory neurotransmission speed up in a dose-dependent fashion by bath application of K^+ as well as 5-HT and NMDA (Bracci et al. 1996b). This suggests that segmental changes in frequency reflect increased excitability of interneuronal networks. Do increases in disinhibited network excitability mean that neurons normally part of the locomotor CPG are also depolarized? While network dynamics are clearly different in the presence of inhibitory connectivity, several lines of evidence suggest that a subpopulation of interneurons are shared between the locomotor and disinhibited networks. First work in the neonatal rat using split bath techniques showed a tight interaction between locomotor-like and disinhibited excitatory rhythm (Beato and Nistri 1999). Second, lesion studies have shown that the ventral quadrant of the spinal cord is sufficient to elicit either the locomotor or the disinhibited pattern of activity (Bracci et al. 1996a). Finally, our calcium imaging data suggest that a majority of retrogradely labeled ventral interneurons are activated during a episode. Interneurons such as those represented in Fig. 2 are commissural interneurons that represent a heterogeneous population of excitatory and inhibitory interneurons that project to interneurons and motoneurons located in the contralateral ventral horn (Lanuza et al. 2004). Based on immunocytochemical and electrophysiological data from the rat and mouse, it is likely that a subpopulation of the ventral commissural interneurons active during burst initiation are also responsible for coordinating synchronous or alternating locomotor activity between hemisegments (Bracci et al. 1996a; Butt and Kiehn 2003; Kjaerulff and Kiehn 1996; Lanuza et al. 2004). Collectively, data from this manuscript along with previous work suggest that episodic activity is most likely due to an increased activity of interneurons leading to increases in network excitability. A caveat is that this does not preclude a possible contribution of motoneurons to generating episodic activity

FIG. 6. Rhythmogenic compounds effectively produce rostrocaudal gradients of excitability. *AI*: neurograms from T_{12} (*top*) and L_5 (*bottom*) ventral roots after bath application of 5 μM *N*-methyl-D(L)-aspartic acid (NMA), 10 μM 5-HT, and 50 μM DA after a transection at L_3. *AII*: neurogram showing rhythmic locomotor-like bursting from L_2 and L_5 ventral roots evoked with 5 μM NMA, 10 μM 5-HT, and 50 μM DA. *BI*: recordings from T_{12} (*top*) and L_5 (*bottom*) ventral roots with 15 μM 5-HT and 75 μM DA after a transection at L_3. *BII*: neurogram showing rhythmic locomotor-like bursting from L_2 and L_5 ventral roots evoked with 15 μM 5-HT and 75 μM DA. *CI*: recordings from T_{12} (*top*) and L_5 (*bottom*) ventral roots with 20 μM D_1, 40 μM D_2, and 4 μM 5-HT_2 receptor agonists after a transection at L_3. *CII*: neurogram showing rhythmic locomotor-like bursting from L_2 and L_5 ventral roots evoked with 20 μM D_1, 40 μM D_2, and 4 μM 5-HT_2 receptor agonists. *DI*: summary plot comparing cycle periods between rostral and caudal segments with NMA, 5-HT, DA ($P < 0.05$, $n = 5$). *DII*: summary plot comparing cycle periods between rostral and caudal segments with 5-HT and DA ($P < 0.05$, $n = 5$). *DIII*: summary plot comparing cycle periods between rostral and caudal segments with D_1, D_2, and 5-HT_2 receptor agonists ($P < 0.05$, $n = 8$).

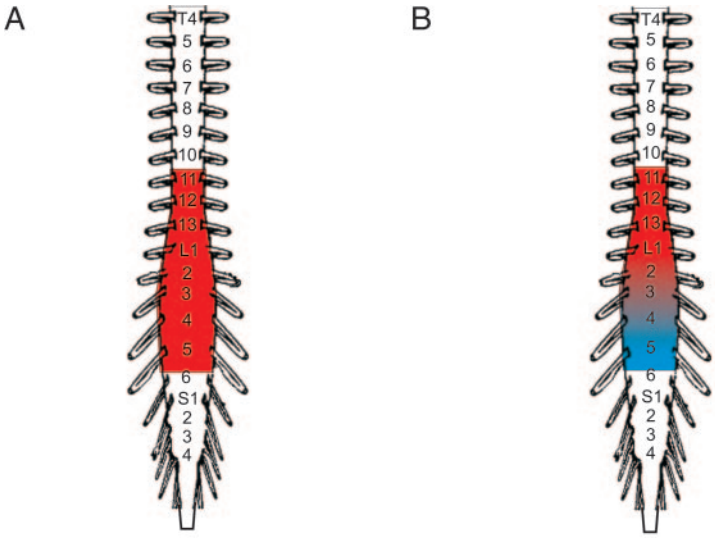

FIG. 7. Summary schematic. *A*: uniform excitability created between T_{11} and L_6 ventral roots when D_1, D_2, 5-HT_2 receptor agonists, and 10 μM 5-HT are bath-applied to the cord. *B*: excitability gradient created when DA, 30 μM 5-HT, and locomotor producing cocktails are added to bath. (Spinal cord schematic adapted from Clarac et al. 2004).

Drug	Bath Concentration
D_1	(20 μM)
D_1/D_2	(20 μM/40 μM)
5-HT_2	(4 μM)
5-HT	(10 μM)

Drug	Bath Concentration
DA	(50 μM and 100μM)
5-HT	(30 μM)
NMA/5-HT/DA	(5 μM/10 μM/50 μM)
5-HT/DA	(15 μM/75 μM)
5-$HT_2/D_1/D_2$	(4 μM/20 μM/40 μM)

through gap junction–mediated systems (Tresch and Kiehn 2000).

Monoaminergic receptor and fiber distribution

The results from this study are generally supported by immunocytochemical work in the neonatal rat and mouse. 5-HT at high concentrations (30 μM) produces a rostrocaudal gradient likely though activation of multiple receptor subtypes (Madriaga et al. 2004). 5-HT_7 receptors seem to be distributed in a rostrocaudal direction in the neonatal rat spinal cord and predominately so in thoracic segments (Cina and Hochman 1998; Schmidt and Jordan 2000). In contrast, 5-HT_{2A} receptors are widely expressed in lumbar regions, which may explain why 5-HT_2 agonists did not produce a rostrocaudal gradient of excitability in our preparation. The data on DA receptor and fiber distribution in neonatal rodents is sparse, but recent data suggest a uniform distribution of D_1 receptors in the mouse (Zhu et al. 2004). This is consistent with our results showing that D_1 agonists increase excitability of network activity uniformly throughout the thoracolumbar spinal cord. Similar to 5-HT, it is likely that DA is acting through multiple receptors such as D_5 and D_3 to modulate or evoke locomotor activity, especially at the doses used. In favor of this idea, combinations of agonists (5-HT_2 and D_1/D_2) that did not produce rostrocaudal gradients when applied in isolation did so when bath-applied concurrently. It is sobering to consider the combinatorial complexity of possible signaling pathways activated pre- and postsynaptically by monoamines (Greengard 2001).

Available data suggest that 5-HT and DA fibers may be distributed in such a way to functionally modify or create rostrocaudal gradients of network activity in the developing spinal cord. Monoaminergic fibers progressively innervate thoracolumbar regions rostrocaudally during development, with fibers being first detected by E15 (Ballion et al. 2002) for 5-HT and E18 for NA (Rajaofetra et al. 1992). Microdialysis data show evidence for release of DA metabolites, as well as 5-HT and NA, in the thoracolumbar ventral horn or funiculus of neonatal and adult rats after exercise or stimulation of the brain stem (Gerin and Privat 1998; Jordan and Schmidt 2002). 5-HT and DA is released after brain stem stimulation in neonatal rats maximally in the $T_{11–13}$ segments with a lower level of release in lumbar segments (Jordan and Schmidt 2002; L. Jordan, personal communication).

Functional relevance

Under more physiological conditions, when an escape-like response is elicited by dorsal root stimulation or mechanical stimulation in mouse spinal cord preparations, a rostrocaudal wave of activity propagates with a 4% segmental phase lag across the rostral lumbar segments (Bonnot et al. 2002a,b). This suggests that rostrocaudal gradients are an emergent property of network activity. An attractive possibility is the generation of rostrocaudal gradients of excitability by bath application of monoamines promotes stable activation of locomotor networks. In the neonatal rat and mouse, bath application of 5-HT, DA, and NMA can activate locomotor networks for extended periods (Bonnot et al. 2002a; Jiang et al. 1999a; Whelan 2003). 5-HT activates locomotor networks (Kiehn and Kjaerulff 1998; Kremer and Lev-Tov 1997), with thoracolumbar segments being more readily activated (Cowley and Schmidt 1997). Interestingly, strategies to uniformly depolarize populations of interneurons in the thoracolumbar spinal cord by increasing extracellular K^+ do not generally produce sustained bouts of locomotor activity (Bracci et al. 1998; unpublished observations). Also, other studies using low Mg^{2+} point to a rostrocaudal organization of locomotor networks, but

notably the rhythm is unstable (Bonnot et al. 1998). On the other hand, rostrocaudal gradients are not the only possibility for the effectiveness of monoamines in activating locomotor networks. 5-HT and DA acting on multiple receptor pathways activate several intracellular signaling pathways that can lead to both inhibition and excitation of neurons (Schmidt and Jordan 2000). Thus it is not surprising that monoamines, especially 5-HT, affect multiple conductances such as K_{leak}, I_h, I_A, and K_{Ca} in motoneurons (Rekling et al. 2000). It also needs to be emphasized that, while rostrocaudal gradients are important in sequencing and activating components of distributed networks, transverse gradients of excitability across the face of the spinal cord are important for CPG function (Kiehn and Kjaerulff 1998). For example, 5-HT_{2A} receptors are localized preferentially in ventral laminae of the spinal cord (Schmidt and Jordan 2000). Approaches using molecular biology techniques to genetically dissect CPG circuits will likely prove useful for examining the effects of monoamines on CPG interneurons (Goulding and Pfaff 2005).

We have not addressed the role of noradrenaline (NA) in generating rostrocaudal gradients in this study, but previously published data suggest that it may preferentially act on sacral segments of the spinal cord through α_1 receptors to produce a fast rhythm that propagates rostrally to activate lumbar segments (Gabbay and Lev-Tov 2004). This creates the scenario of modulation of rostrocaudal gradients by selective release of DA, 5-HT, or NA. In turn, this could contribute to differential control of segmental components consistent with the unit burst oscillator hypothesis (Grillner 1981). While rostrocaudal gradients have been observed in adult cats, it is not clear whether network dynamics are comparable between species (Bonnot et al. 2002b; Yakovenko et al. 2002). It is likely that at least part of the monoaminergic gradients of excitability may be a function of developmental maturation of networks (Bonnot and Morin 1998; Bonnot et al. 1998).

In summary, our results show that bath combinations of rhythmogenic drugs that activate locomotor networks generate rostrocaudal gradients of excitability. We hypothesize that these gradients of excitability set up a permissive environment for the emergence of locomotor networks in neonatal preparations. This could be one mechanism by which these combinations of monoaminergic compounds can stably activate locomotor networks.

ACKNOWLEDGMENTS

We acknowledge the excellent technical assistance of M. Tran.

GRANTS

This research was supported by the Canadian Institutes of Health Research, and the Heart and Stroke Foundation of Canada. K. J. Christie was supported by a National Sciences and Engineering Research Council Postgraduate scholarship-studentship.

REFERENCES

Ballion B, Branchereau P, Chapron J, and Viala D. Ontogeny of descending serotonergic innervation and evidence for intraspinal 5-HT neurons in the mouse spinal cord. *Brain Res Dev Brain Res* 137: 81–88, 2002.

Barriere G, Mellen N, and Cazalets JR. Neuromodulation of the locomotor network by dopamine in the isolated spinal cord of newborn rat. *Eur J Neurosci* 19: 1325–1335, 2004.

Beato M and Nistri A. Interaction between disinhibited bursting and fictive locomotor patterns in the rat isolated spinal cord. *J Neurophysiol* 82: 2029–2038, 1999.

Bertrand S and Cazalets JR. The respective contribution of lumbar segments to the generation of locomotion in the isolated spinal cord of newborn rat. *Eur J Neurosci* 16: 1741–1750, 2002.

Bonnot A, Mentis GZ, Skoch J, and O'Donovan MJ. Electroporation loading of calcium-sensitive dyes into the CNS. *J Neurophysiol* 93: 1793–1808, 2005.

Bonnot A and Morin D. Hemisegmental localisation of rhythmic networks in the lumbosacral spinal cord of neonate mouse. *Brain Res* 793: 136–148, 1998.

Bonnot A, Morin D, and Viala D. Genesis of spontaneous rhythmic motor patterns in the lumbosacral spinal cord of neonate mouse. *Brain Res Dev Brain Res* 108: 89–99, 1998.

Bonnot A, Whelan PJ, Mentis GZ, and O'Donovan MJ. Locomotor-like activity generated by the neonatal mouse spinal cord. *Brain Res Brain Res Rev* 40: 141–151, 2002a.

Bonnot A, Whelan PJ, Mentis GZ, and O'Donovan MJ. Spatiotemporal pattern of motoneuron activation in the rostral lumbar and the sacral segments during locomotor-like activity in the neonatal mouse spinal cord. *J Neurosci* 22: RC203, 2002b.

Bracci E, Ballerini L, and Nistri A. Localization of rhythmogenic networks responsible for spontaneous bursts induced by strychnine and bicuculline in the rat isolated spinal cord. *J Neurosci* 16: 7063–7076, 1996a.

Bracci E, Ballerini L, and Nistri A. Spontaneous rhythmic bursts induced by pharmacological block of inhibition in lumbar motoneurons of the neonatal rat spinal cord. *J Neurophysiol* 75: 640–647, 1996b.

Bracci E, Beato M, and Nistri A. Afferent inputs modulate the activity of a rhythmic burst generator in the rat disinhibited spinal cord in vitro. *J Neurophysiol* 77: 3157–3167, 1997.

Bracci E, Beato M, and Nistri A. Extracellular K^+ induces locomotor-like patterns in the rat spinal cord in vitro: comparison with NMDA or 5-HT induced activity. *J Neurophysiol* 79: 2643–2652, 1998.

Butt SJ and Kiehn O. Functional identification of interneurons responsible for left-right coordination of hindlimbs in mammals. *Neuron* 38: 953–963, 2003.

Christie KJ and Whelan PJ. Dopamine contributes to the formation of a rostrocaudal gradient of spinal rhythmic excitability. *Soc Neurosci Abstr* 883–886, 2004.

Cina C and Hochman S. Serotonin receptor pharmacology of the mammalian locomotor CPG: Activation by a 5-HT receptor agonist in the isolated rat spinal cord. *Soc Neurosci Abstr* 24: 654–624, 1998.

Clarac F, Pearlstein E, Pflieger JF, and Vinay L. The in vitro neonatal rat spinal cord preparation: a new insight into mammalian locomotor mechanisms. *J Comp Physiol A* 190: 343–357, 2004.

Cohen AH. Effects of oscillator frequency on phase-locking in the lamprey central pattern generator. *J Neurosci Methods* 21: 113–125, 1987.

Cowley KC and Schmidt BJ. Effects of inhibitory amino acid antagonists on reciprocal inhibitory interactions during rhythmic motor activity in the in vitro neonatal rat spinal cord. *J Neurophysiol* 74: 1109–1117, 1995.

Cowley KC and Schmidt BJ. Regional distribution of the locomotor pattern-generating network in the neonatal rat spinal cord. *J Neurophysiol* 77: 247–259, 1997.

Gabbay H and Lev-Tov A. Alpha-1 adrenoceptor agonists generate a "fast" NMDA receptor-independent motor rhythm in the neonatal rat spinal cord. *J Neurophysiol* 92: 997–1010, 2004.

Gerin C and Privat A. Direct evidence for the link between monoaminergic descending pathways and motor activity: II. A study with microdialysis probes implanted in the ventral horn of the spinal cord. *Brain Res* 794: 169–173, 1998.

Goulding M and Pfaff SL. Development of circuits that generate simple rhythmic behaviors in vertebrates. *Curr Opin Neurobiol* 15: 14–20, 2005.

Greengard P. The neurobiology of slow synaptic transmission. *Science* 294: 1024–1030, 2001.

Grillner S. Control of locomotion in bipeds, tetrapods, and fish. In: *Handbook of Physiology—The nervous system*, edited by Geiger SR, Brooks VB, Brookhart JM, and Mountcastle VB. Baltimore, MD: Waverly Press, 1981, p. 1179–1236.

Grillner S. The motor infrastructure: from ion channels to neuronal networks. *Nat Rev Neurosci* 4: 573–586, 2003.

Hagevik A and McClellan AD. Coordination of locomotor activity in the lamprey: role of descending drive to oscillators along the spinal cord. *Exp Brain Res* 128: 481–490, 1999.

Iizuka M. Rostrocaudal distribution of spinal respiratory motor activity in an in vitro neonatal rat preparation. *Neurosci Res* 50: 263–269, 2004.

Jiang Z, Carlin KP, and Brownstone RM. An in vitro functionally mature mouse spinal cord preparation for the study of spinal motor networks. *Brain Res* 816: 493–499, 1999a.

Jiang Z, Rempel J, Li J, Sawchuk MA, Carlin KP, and Brownstone RM. Development of L-type calcium channels and a nifedipine-sensitive motor activity in the postnatal mouse spinal cord. *Eur J Neurosci* 11: 3481–3487, 1999b.

Jordan LM and Schmidt BJ. Propriospinal neurons involved in the control of locomotion: potential targets for repair strategies? *Prog Brain Res* 137: 125–139, 2002.

Kiehn O and Kjaerulff O. Distribution of central pattern generators for rhythmic motor outputs in the spinal cord of limbed vertebrates. *Ann NY Acad Sci* 860: 110–129, 1998.

Kiemel T, Gormley KM, Guan L, Williams TL, and Cohen AH. Estimating the strength and direction of functional coupling in the lamprey spinal cord. *J Comput Neurosci* 15: 233–245, 2003.

Kjaerulff O and Kiehn O. Distribution of networks generating and coordinating locomotor activity in the neonatal rat spinal cord in vitro: a lesion study. *J Neurosci* 16: 5777–5794, 1996.

Kremer E and Lev-Tov A. Localization of the spinal network associated with generation of hindlimb locomotion in the neonatal rat and organization of its transverse coupling system. *J Neurophysiol* 77: 1155–1170, 1997.

Lanuza GM, Gosgnach S, Pierani A, Jessell TM, and Goulding M. Genetic identification of spinal interneurons that coordinate left-right locomotor activity necessary for walking movements. *Neuron* 42: 375–386, 2004.

Madriaga MA, McPhee LC, Chersa T, Christie KJ, and Whelan PJ. Modulation of locomotor activity by multiple 5-HT and dopaminergic receptor subtypes in the neonatal mouse spinal cord. *J Neurophysiol* 92: 1566–1576, 2004.

Matsushima T and Grillner S. Intersegmental co-ordination of undulatory movements—a "trailing oscillator" hypothesis. *Neuroreport* 1: 97–100, 1990.

Matsushima T and Grillner S. Neural mechanisms of intersegmental coordination in lamprey: local excitability changes modify the phase coupling along the spinal cord. *J Neurophysiol* 67: 373–388, 1992.

Nishimaru H, Takizawa H, and Kudo N. 5-Hydroxytryptamine-induced locomotor rhythm in the neonatal mouse spinal cord in vitro. *Neurosci Lett* 280: 187–190, 2000.

O'Donovan MJ. The origin of spontaneous activity in developing networks of the vertebrate nervous system. *Curr Opin Neurobiol* 9: 94–104, 1999.

O'Donovan MJ, Ho S, Sholomenko G, and Yee W. Real-time imaging of neurons retrogradely and anterogradely labelled with calcium-sensitive dyes. *J Neurosci Methods* 46: 91–106, 1993.

Rajaofetra N, Poulat P, Marlier L, Geffard M, and Privat A. Pre- and postnatal development of noradrenergic projections to the rat spinal cord: an immunocytochemical study. *Brain Res Dev Brain Res* 67: 237–246, 1992.

Rekling JC, Funk GD, Bayliss DA, Dong XW, and Feldman JL. Synaptic control of motoneuronal excitability. *Physiol Rev* 80: 767–852, 2000.

Roberts A and Tunstall MJ. Longitudinal gradients in the spinal cord of Xenopus embryos and their possible role in coordination of swimming. *Eur J Morphol* 32: 176–184, 1994.

Schmidt BJ and Jordan LM. The role of serotonin in reflex modulation and locomotor rhythm production in the mammalian spinal cord. *Brain Res Bull* 53: 689–710, 2000.

Smith JC, Feldman JL, and Schmidt BJ. Neural mechanisms generating locomotion studied in mammalian brain stem-spinal cord in vitro. *FASEB J* 2: 2283–2288, 1988.

Sqalli-Houssaini Y and Cazalets JR. Noradrenergic control of locomotor networks in the in vitro spinal cord of the neonatal rat. *Brain Res* 852: 100–109, 2000.

Sqalli-Houssaini Y, Cazalets JR, and Clarac F. Oscillatory properties of the central pattern generator for locomotion in neonatal rats. *J Neurophysiol* 70: 803–813, 1993.

Tresch MC and Kiehn O. Motor coordination without action potentials in the mammalian spinal cord. *Nat Neurosci* 3: 593–599, 2000.

Tunstall MJ and Roberts A. A longitudinal gradient of synaptic drive in the spinal cord of Xenopus embryos and its role in co-ordination of swimming. *J Physiol* 474: 393–405, 1994.

Wenner P and O'Donovan MJ. Mechanisms that initiate spontaneous network activity in the developing chick spinal cord. *J Neurophysiol* 86: 1481–1498, 2001.

Whelan P, Bonnot A, and O'Donovan MJ. Properties of rhythmic activity generated by the isolated spinal cord of the neonatal mouse. *J Neurophysiol* 84: 2821–2833, 2000.

Whelan PJ. Developmental aspects of spinal locomotor function: insights from using the in vitro mouse spinal cord preparation. *J Physiol* 553: 695–706, 2003.

Yakovenko S, Mushahwar V, VanderHorst V, Holstege G, and Prochazka A. Spatiotemporal activation of lumbosacral motoneurons in the locomotor step cycle. *J Neurophysiol* 87: 1542–1553, 2002.

Zhu H, Sawchuk MA, Clemens S, and Hochman S. Distribution of D1-D5 dopamine receptor mRNA in mouse spinal cord. *Soc Neurosci Abstr* 2004: 656–615, 2004.